

## OR2-7

ISS-ELF で溶融凝固させた TiC 添加 Ti-6Al-4V 試料  
における SPring-8 の XRD-CT を用いた粒数推定Estimating Number of Grains of TiC Added Ti-6Al-4V  
Sample Melted and Solidified in the ISS-ELF  
Using XRD-CT at SPring-8

門井洸衛<sup>1\*</sup>, 櫛舎祐太<sup>1</sup>, 上野遥か<sup>1</sup>, 市川文彩<sup>1</sup>, 小林正和<sup>2</sup>, 山田素子<sup>3</sup>, 佐藤尚<sup>3</sup>, 渡辺義見<sup>3</sup>, 中野禪<sup>4</sup>, 鈴木進補<sup>1</sup>

Koei KADOI<sup>1</sup>, Yuta KUSHIYA<sup>1</sup>, Haruka UENO<sup>1</sup>, Aya ICHIKAWA<sup>1</sup>, Masakazu KOBAYASHI<sup>2</sup>,  
Motoko YAMADA<sup>3</sup>, Hisashi SATO<sup>3</sup>, Yoshimi WATANABE<sup>3</sup>, Shizuka NAKANO<sup>4</sup>,  
and Shinsuke SUZUKI<sup>1</sup>

<sup>1</sup> 早稲田大学, Waseda University,

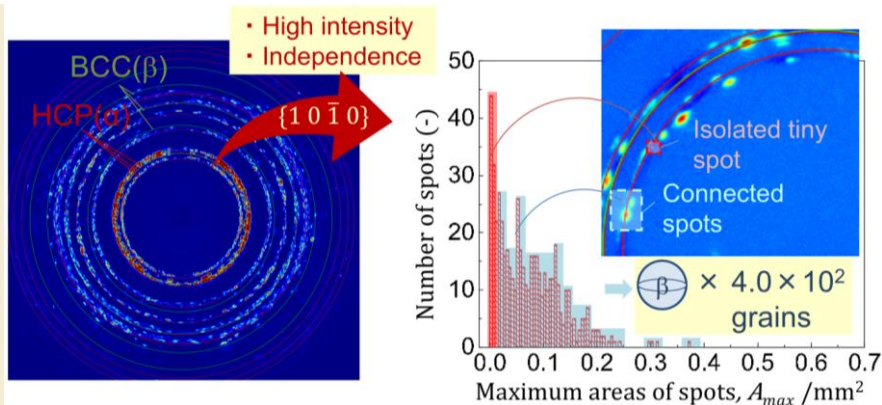
<sup>2</sup> 豊橋技術科学大学, Toyohashi University of Technology,

<sup>3</sup> 名古屋工業大学, Nagoya Institute of Technology,

<sup>4</sup> 株式会社 Henry Monitor, Henry Monitor Inc.

\* Correspondence: kadoikouei2000@toki.waseda.jp

**Abstract:** The objective of this study was to establish a method of estimating the number of prior- $\beta$  grains in Ti-6Al-4V of the ISS-ELF samples refined by TiC heterogeneous nucleation site particles using XRD patterns obtained at SPring-8 BL20XU. The X-ray wavelength was  $3.28 \times 10^{-14}$  m and the detector



distance was 51 mm. The sample was rotated by  $0.5^\circ$  steps. As a result, 720 diffraction patterns were obtained for  $360^\circ$ . For analysis, 360 symmetry-equivalent patterns were used. For each pixel, the median intensity,  $I_0$ , over 360 frames was taken as background and signal was extracted as  $\log(I/I_0)$ . High-intensity, non-overlapping spots on the  $\{1\ 0\ \bar{1}\ 0\}$  ring of  $\alpha$  phase were selected. Spots that centroids overlapped across consequent frames were grouped. The maximum projected area of each group was taken as representative value. The unit of the area was converted to  $\text{mm}^2$  from pixels as  $A_{\max}$ . Groups with  $A_{\max}$  of  $0.0151\ \text{mm}^2$  or larger were assigned to  $\beta$  grains. The mean  $A_{\max}$  corresponded to a sphere-equivalent volume of  $1.5 \times 10^{-2}\ \text{mm}^3$ . Dividing the sample volume of  $6.0\ \text{mm}^3$  by this volume, the number of  $\beta$  grains was estimated  $4.0 \times 10^2$ . This results agreed with the results of Voronoi tessellation method.

**Keywords:** Ti-6Al-4V, TiC, Heterogenous nucleation site particles, Number of grains, X-ray diffraction, SPring-8, BL20XU, Image analysis, ISS-ELF, Hetero-3D

## 1. Introduction

Addition of TiC heterogeneous nucleation site particles refine the prior- $\beta$  grains which are primary crystal of Ti-6Al-4V<sup>1)</sup> before the phase transformation to  $\alpha$  phase. To evaluate only the amount of TiC acting as nucleation sites, *Hetero-3D* mission was conducted by melting and solidifying samples in the electrostatic levitation furnace in the International Space Station (ISS-ELF)<sup>2)</sup>. Due to the limited number of space experimental samples, X-ray diffraction (XRD) with synchrotron beam line in SPring-8 was conducted as the non-destructive method for estimating the number of  $\beta$  grains in the entire sample. This study aims to establish the method of estimating the number of prior- $\beta$  grains from XRD patterns of the ISS-ELF sample.

## 2. Experimental Procedures

Ti-6Al-4V with TiC 5 mass% was melted and solidified in the ISS-ELF. The experiment was conducted under the heating condition<sup>3)</sup> for remaining TiC contributes to refine grains. XRD was performed using BL20XU at SPring-8. The X-ray wavelength was  $3.28 \times 10^{-14}$  m, and the distance between the sample and the detector was 51 mm. An image of a diffraction pattern was obtained for every 0.5 degrees of sample rotation angle,  $\omega$ , for a total of 720 diffraction patterns covering 360 degrees of rotation. The diffraction patterns consisted of  $2048 \times 2048$  pixels.

Due to rotation symmetry, only the 360 images from the  $1^\circ$  to the  $180^\circ$  were used. For each image, the intensity,  $I$ , was recorded for each pixel coordinate. For a background filter, the median intensity,  $I_0$ , as a constant signal derived from the experimental system was taken for each pixel coordinate from the 360 images. To detect significant signals relative to the background signal on both the low and high sides of the absolute intensity value, the logarithmic difference,  $\log(I/I_0)$ , was calculated. The value of  $\log(I/I_0)$  was plotted as a diffraction pattern.  $\alpha$  grains with an HCP structure had the potential to be detected as diffraction spots on 13 different crystal planes. On the other hand,  $\beta$  grains with a BCC structure had the potential to be detected as diffraction spots on four different crystal planes. Using Bragg's law, the diffraction angle  $2\theta$  corresponding to each crystal plane was calculated, and diffraction rings were drawn.

## 3. Results

The diffraction pattern with overlapping diffraction rings is shown in **Fig. 1(a)**. The ring corresponding to the  $\{1\ 0\ \bar{1}\ 0\}$  plane maintained significant intensity relative to the background and did not overlap with other rings.

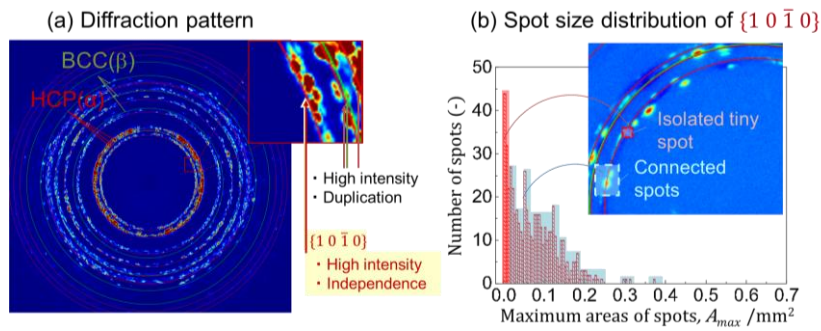


**Figure 1.** Diffraction pattern of the sample with refined  $\beta$  grain. (a) shows red rings and green rings as the diffraction rings of  $\alpha$  grains with HCP structure and  $\beta$  grains with BCC structure, respectively. (b) shows the area histogram of the diffraction spots of the  $\{1\ 0\ \bar{1}\ 0\}$  plane, which was judged to be the best diffraction ring in (a).

## 4. Discussion

From the definition of  $\omega$ , spots in the diffraction pattern with consecutive frame numbers have close spatial coordinates in the crystal. Furthermore, the azimuth angle of the spot on a diffraction pattern depends on the direction relative to the sample coordinate system of the crystal plane. Therefore, it can be considered that the diffraction spots of  $\alpha$  grains connected in the diffraction pattern belonged to the same  $\beta$  grain before the phase transformation. Therefore, the continuous diffraction spots around 26-neighborhood defined as a single spot. The maximum area of a spot with the unit of pixels that appeared in the continuous frames was taken as the representative value. This value can be converted to the maximum projected area of the grain,

$A_{\max}$  with the unit of  $\text{mm}^2$  by the detector pixel size of 1 px of 0.019 mm. Isolated spots smaller than  $0.012 \text{ mm}^2$  within the group were data defects and were removed by a 1-boxel expansion-contraction process. The histogram of  $A_{\max}$  for diffraction spots after noise processing is shown in **Fig. 1(b)**.

In **Fig. 1(b)**, groups with  $A_{\max} \geq 0.0151 \text{ mm}^2$ , where diffraction spots are connected, were regarded as  $\beta$  grains. The average area in this range was calculated to be  $9.5 \times 10^{-2} \text{ mm}^2$ . This value was converted to a spherical equivalent volume of  $1.5 \times 10^{-2} \text{ mm}^3$  and divided by the sample volume of  $6.0 \text{ mm}^3$  to estimate the number of particles in the refined sample to be  $4.0 \times 10^2$  particles. This result was consistent with the number estimation results<sup>2)</sup> obtained using the Voronoi tessellation (VT) method for the same sample.

## 5. Conclusions

Rotation XRD patterns were measured at SPring-8 (BL20XU). For each pixel, the median intensity  $I_0$  from 360 frames was taken as the background. The signal was computed as  $\log(I/I_0)$ . High-intensity, non-overlapping spots on the  $\{10\bar{1}0\}$  diffraction ring were selected. Spots whose centroids overlapped in consecutive frames were grouped. For each group, the maximum projected area was taken as the representative value. Groups with  $A_{\max} \geq 0.0151 \text{ mm}^2$  were counted as prior- $\beta$  grains. The mean  $A_{\max}$  was converted to a sphere-equivalent volume. Dividing the sample volume by this volume yielded  $4.0 \times 10^2$  grains. This estimate agreed with VT for the same sample.

## Acknowledgments

This study was conducted as the experiments for *Hetero-3D* mission, using the Japanese Experiment Module, “Kibo”, on the ISS. ISS-ELF experiments were conducted with the help of Prof. T. Ishikawa, Dr. C. Koyama, Mr. H. Oda, and Mr. Y. Watanabe belonging to Japan Aerospace Exploration Agency (JAXA). The synchrotron radiation experiments were performed at the BL20XU at SPring-8 with the approval of JASRI (proposal nos. 2024B1125). This work was supported by JST SPRING, Grant Number JPMJSP2128, by Waseda University Special Research Project 2024C-708. Furthermore, we would like to thank Kimura Foundry Co., Ltd. for their financial support.

## Conflicts of Interest

The authors declare no conflict of interest.

## Nomenclature

$\omega$	Rotation angle of a sample in X-ray diffraction experiment system (deg)
$2\theta$	Diffraction angle (deg)
$I$	Intensity of diffraction spots (-)
$I_0$	Median intensity of diffraction spots in the same coordination (-)
$A_{\max}$	Maximum projected area of grain ( $\text{mm}^2$ )

## References

- 1) Y. Watanabe, M. Sato, T. Chiba, H. Sato, N. Sato and S. Nakano: 3D visualization of top surface structure and pores of 3D printed Ti-6Al-4V samples manufactured with TiC heterogeneous nucleation site particles. *Metall. Mater. Trans. A*, **51** (2019) 1345, DOI: <https://doi.org/10.1007/s11661-019-05597-z>.
- 2) K. Kadoi, C. Hanada, Y. Mabuchi, Y. Ueda, Y. Kushiya, H. Aoki, K. Yoneda, R. Saguchi, M. Yamada, H. Sato, Y. Watanabe, S. Nakano and S. Suzuki: Proceedings of the 75th International Astronautical Congress, Milan, Italy (2024), IAC-24-A2.6.7. DOI: <https://doi.org/10.52202/078356-0040>.
- 3) Y. Mabuchi, H. Aoki, C. Hanada, Y. Ueda, K. Kadoi, Y. Kushiya, R. Saguchi, K. Yoneda, M. Yamada, H. Sato, Y. Watanabe, S. Ozawa, S. Nakano, C. Koyama, H. Oda, T. Ishikawa, Y. Watanabe, T. Shimaoka and S. Suzuki: Heating conditions in electrostatic levitation experiments for grain refinement of Ti-6Al-4V with TiC. *Int. J. Microgravity Sci. Appl.*, **41** (2024) 410201, DOI: <https://doi.org/10.15011/jasma.41.410201>.



© 2025 by the authors. Submitted for possible open access publication under the terms and conditions of the Creative Commons Attribution (CC BY) license (<http://creativecommons.org/licenses/by/4.0/>).